

SEARCH STRATEGIES FOR HIGGS BOSONS AT HIGH ENERGY e^+e^- COLLIDERS*

J. ALEXANDER,^(a) D. L. BURKE, C. K. JUNG, S. KOMAMIYA

Stanford Linear Accelerator Center, Stanford University, Stanford, California 94309

P. R. BURCHAT

Santa Cruz Institute for Particle Physics, University of California, Santa Cruz, California 95064

ABSTRACT

We have used detailed Monte Carlo simulations to study search strategies for Higgs bosons at high energy e^+e^- colliders. We extend an earlier study of the minimal single-Higgs-doublet model at a center-of-mass energy of 1 TeV to examine the effects of b -quark tagging and jet counting. It is found that these techniques can increase the signal-to-noise ratio substantially in the mass range around the W mass. In addition, we have studied this model at a center-of-mass energy of 400 GeV and found that an e^+e^- collider in this region would be sensitive to a Higgs boson with mass up to twice the Z^0 mass.

We have also considered a nonminimal two-doublet model for the Higgs sector by extending a study of charged Higgs boson searches to include a mass very close to the mass of the W^\pm . We demonstrate that techniques which include b -quark tagging can be utilized to extract a significant signal. In addition, we have examined the prospects for detecting nonminimal neutral Higgs bosons at 1 TeV. We conclude that it would be possible to detect the CP-even and CP-odd neutral Higgs bosons when they are pair-produced in e^+e^- annihilation over a limited mass range. However, in some scenarios of supersymmetry, the charged Higgs boson constitutes a significant background to the CP-odd and the more massive CP-even neutral Higgs boson.

1. INTRODUCTION

We continue two earlier studies of Higgs boson search strategies at a 1 TeV e^+e^- collider: one for the neutral boson H^0 which remains as a physical particle in the minimal Higgs theory,¹⁾ and another for the charged bosons H^\pm which appear in two-doublet versions of the Higgs sector.²⁾ These studies included the effects of detector resolution on the observed final states and of beamstrahlung on the spectrum of center-of-mass energies at which e^+e^- collisions take place. The main conclusions of the previous studies were the following:

*Work supported by Department of Energy, contracts DE-AC03-76SF00515 and DE-AM03-76SF00010.

^(a)Present address: Cornell University, Ithaca, New York 14853.

- It is possible to extract a significant signal from all standard model backgrounds if the mass of the minimal Higgs boson is not near the mass of the W^\pm or Z^0 and is less than 400 (500) GeV when a data sample of 10 (30) fb^{-1} has been collected at 1 TeV. The most important signal is due to the process $e^+e^- \rightarrow \nu_e \bar{\nu}_e H^0$. In the region around the mass of the W^\pm , the major background to this signal is due to the process $e^+e^- \rightarrow e^+ \nu_e W^-$.
- Production of a charged Higgs boson with mass less than about 80% of the beam energy is detectable with an integrated luminosity of about 10 fb^{-1} at 1 TeV through direct pair production and also from the decay of the top quark if the top quark is massive enough. In this study, charged Higgs bosons with mass less than about 100 GeV were not considered.

In this paper, we extend the above studies in the following ways:

- For the minimal Higgs boson at $\sqrt{s} = 1$ TeV, we consider b -quark tagging and jet counting as ways to enhance the signal at M_{H^0} near M_{W^\pm} .
- We study search strategies for the minimal Higgs boson at $\sqrt{s} = 400$ GeV.
- We study the detection of nonminimal neutral Higgs bosons through the pair production of a CP-even and CP-odd neutral Higgs boson at $\sqrt{s} = 1$ TeV.
- For the charged Higgs boson, we consider b -quark tagging, as well as other techniques, to enhance the signal around the mass of the W^\pm .

2. SIMULATION OF EVENTS AND DETECTOR RESPONSE

We have used standard Monte Carlo techniques to generate both signal and background events, and to simulate the response of the detector. Detailed accounts of these simulations are given in Refs. (1) and (2), but we briefly review them here.

2.1 Beamstrahlung

The extremely high density to which beam particles must be focused to produce sufficient luminosity to do particle physics at a high-energy e^+e^- collider results in a significant interaction rate between the particles of one

beam and the collective electromagnetic fields produced by the particles in the opposite beam. A major consequence of this is that the spectrum of center-of-mass energies at which e^+e^- interactions take place is not at all monochromatic. Radiation of photons during the beam-beam collision ("beamstrahlung") will result in a spectrum of particle interactions that depends in detail on the energy and bunch characteristics of each beam. We have used a spectrum that has been calculated³⁾ for a specific set of beam parameters, but that is typical of most machine designs that have been studied.⁴⁾ This calculation includes the effects of multiple radiation and beam-beam disruption for an e^+e^- machine operating at a nominal center-of-mass energy of 1 TeV and a luminosity of $3 \times 10^{33} \text{ cm}^{-2}\text{s}^{-1}$. Approximately 30% of the luminosity lies within 2% of the nominal center-of-mass energy squared for the spectrum that we have chosen.

Included in the Monte Carlo simulations are both the effective reduction in center-of-mass energy and the net longitudinal momentum created by the energy loss of each beam. The mean fractional energy loss that particles undergo during the beam-beam collision is 0.26 for the spectrum that we have used. We compute production cross sections by convoluting the luminosity spectrum with each cross section evaluated at the reduced center-of-mass energy of individual e^+e^- pairs.

2.2 Event Simulation

With the exception of the Higgs particles that we are studying, we have assumed that the standard model with three generations of quarks and leptons is a correct description of nature. The LUND 6.3 model⁵⁾ with full showering of quark and gluon partons has been used to generate QCD background events and to fragment into hadrons final-state quarks and gluons in all signal and background processes. The mass of the top quark was assumed to be 40 GeV, unless otherwise specified, and the masses of the W^\pm and Z^0 gauge bosons have been taken to be 83 GeV and 93 GeV, respectively. The background process $e^+e^- \rightarrow e^+ \nu_e W^-$ was generated with the formulae of Gabrielli.⁶⁾

2.3 Detector Simulation

The properties of a detector that are necessary to successfully carry out a search for a Higgs boson at a high energy e^+e^- collider are easily achievable with current technology. The emphasis in our analysis is on calorimetry and we generally ignore tracking information for hadrons.

To simulate finite detector resolutions and segmentation we modify the generated particle momenta for signal and background processes in the following manner. We assume the azimuthal and polar angles of muons and electrons are well determined by a tracking chamber. The energy of each muon is smeared by a Gaussian distribution with standard deviation

$$\frac{\sigma_E}{E} = 3 \times 10^{-4} E \text{ GeV}^{-1}$$

This resolution should be achievable, for example, with a drift chamber with radius 1.8 m, 72 position measurements each with 200 μm resolution, and embedded in a solenoidal magnetic field of 1.0 Tesla. For electrons, we calculate

the above smearing for low energies and the calorimetric formula

$$\frac{\sigma_E}{E} = \frac{8\%}{\sqrt{E}} \text{ GeV}^{1/2} + 2\%$$

for high energies, and apply the smearing formula which gives the best resolution for a particular energy. We assume that the charges of electrons and muons can be assigned unambiguously.

Photons and charged and neutral hadrons are treated indiscriminately as clusters of calorimetric energy. Tracks within 4° of one another are combined; then the direction of the combined track is smeared by a box function of size $\pm 2^\circ$. The energies of these tracks are smeared with

$$\frac{\sigma_E}{E} = \frac{50\%}{\sqrt{E}} \text{ GeV}^{1/2} + 2\%$$

Finally, to account for possible obstruction of the acceptance of the detector near the beam line by machine components and the hardware needed to support them, we simply ignore particles within 10° of the beam axis. We assume, however, that the remainder of the detector is completely hermetic, and that the hardware performs well enough to avoid any further loss of sensitivity to the presence of particles in signal or background events.

2.4 Impact Parameter Tagging

Because Higgs bosons are expected to decay preferentially through b -quarks, the detection of the presence of b -quarks in an event is an important tag which can be used to isolate the production of Higgs particles. The relatively long lifetime of the b -quark gives rise to decay vertices displaced from the primary e^+e^- vertex or, equivalently, to tracks with large impact parameters. At a TeV linear collider, where the uncertainty in the position of the primary vertex is expected to be much smaller than the mean decay length of the b -quark, especially in the plane perpendicular to the beam direction,⁷⁾ precision vertex detectors may be used to identify such large-impact-parameter tracks which can then be exploited to enhance the signal-to-background ratio in searches for Higgs bosons.

We investigate this possibility by simulating the performance of a combined vertex detector and central tracking chamber in our Monte Carlo and using the impact parameter information in the analysis. The simulation is kept simple and generic in order that the success of the analysis not be dependent on specific details of detector design. Each track in an event is projected into the plane transverse to the beam line and the impact parameter is defined as the distance of closest approach of the track projection to the primary vertex. We compute it for each track using the generated four-vectors, and smear these calculated values with an impact parameter resolution function chosen to be $\sigma = \sqrt{A^2 + (B/p)^2}$. The details of the vertex and tracking system are encompassed in the parameters A and B , which reflect in turn the intrinsic resolution of the tracking system and the effect of multiple scattering of particles as they traverse the beam pipe and detector. We choose values of A and B that are characteristic of combined vertex and tracking systems currently in use, namely $A = 5 \mu\text{m}$ and $B = 50 \mu\text{m GeV}$. We assume that the uncertainty in the location of the collision point is small compared to the

impact parameter resolution. For the analysis in this paper, a charged track is defined to be a 'high impact parameter track' if it lies within $|\cos \theta| \leq 0.9$ and has a (smeared) impact parameter less than 3 mm and greater than three times the resolution $\sigma = \sqrt{A^2 + (B/p)^2}$. The 3 mm upper limit suppresses contamination from K_S and Λ decays.

3. MINIMAL HIGGS BOSON AT $\sqrt{s} = 1$ TeV

In Ref. (1), two production mechanisms were considered for the standard model Higgs boson: $e^+e^- \rightarrow Z^0 H^0$ and $e^+e^- \rightarrow \nu_e \bar{\nu}_e H^0$. It was found that the process $e^+e^- \rightarrow \nu_e \bar{\nu}_e H^0$ gave the strongest signal at $\sqrt{s} = 1$ TeV. The signal is well above standard model backgrounds* everywhere except around the mass of the W^\pm (50–150 GeV). In this region, the signal is dominated by the W^\pm mass peak from the process $e^+e^- \rightarrow e^+ \nu_e W^-$ when no attempt is made to enhance the signal through b -quark tagging or jet counting. We will now consider the effect of b -quark tagging and jet counting for the intermediate mass Higgs ($M_H < 2M_W$) at $\sqrt{s} = 1$ TeV.

First, we will review the selection criteria discussed in detail in Ref. (1). We assume that a Higgs boson with mass less than twice M_W will decay to either a top or bottom quark pair depending on the masses of the Higgs boson and the top quark. The philosophy of our analysis of the $e^+e^- \rightarrow \nu_e \bar{\nu}_e H^0$ reaction with $M_H < 2M_W$ is to search for events that contain two acoplanar jets each with mass below that of the W . We select events in which $|\cos \theta_{thr}| < 0.7$ and $|\cos \theta_{miss}| < 0.9$ where θ_{thr} and θ_{miss} are the polar angles of the thrust axis and the missing momentum in the event, respectively. The first cut ensures that the event is well contained in the detector and preferentially rejects processes with differential cross sections which are sharply peaked along the beam axis (for example, $e^+e^- \rightarrow W^+W^-$, $e^+e^- \rightarrow Z^0Z^0$, and $e^+e^- \rightarrow q\bar{q}$). The second cut reduces backgrounds due to events with large beamstrahlung radiation and/or missing particles. We reject events if the visible energy is less than 100 GeV or greater than 400 GeV. This cut removes backgrounds but is extremely efficient for retaining the signal events.

We divide the event into two clusters using a clustering algorithm and select events in which the acoplanarity of the clusters is greater than 10° and in which each cluster has an invariant mass greater than 1 GeV (to reject leptonic decays of the W^\pm) and less than 50 GeV. Finally, events are accepted only if the missing momentum transverse to the beam is greater than 50 GeV and the number of charged particles outside the 10° hole around the beam axis is between 10 and 36. The probability that an event of the type $e^+e^- \rightarrow \nu_e \bar{\nu}_e H^0$ will pass the above selection

*In a CERN study⁸⁾ of detection of neutral heavy Higgs bosons at CLIC ($\sqrt{s} = 2$ TeV), it was found that a significant background to a heavy Higgs boson signal ($M_H \gtrsim 500$ GeV) is due to the process $e^+e^- \rightarrow e^- \bar{\nu}_e Z^0 W^+$. This background was not considered in Ref. 1; however, this background is not as significant for $M_H \lesssim 500$ GeV (the mass range considered in Ref. 1) because the width of the Higgs scales as M_H^3 , leading to a considerably narrower signal at smaller masses. We estimate the contribution from this background⁹⁾ at 10% of the signal for $M_H = 300$ GeV and 20% for $M_H = 500$ GeV in the Weizsacker-Williams approximation with beamstrahlung neglected. This increases to $\sim 40\%$ when the beamstrahlung spectrum described in Sec. 2.1 is included, due to γW interactions involving the beamstrahlung photon.

criteria varies between about 35% and 50% depending on the mass of the Higgs boson and the decay mode of the Higgs boson. The background is dominated by the process $e^+e^- \rightarrow e^+ \nu_e W^-$. When the invariant mass of the event is plotted in 4 GeV bins the peak bin for the background distribution contains about 25 to 50 times as many events as the peak bin for the signal. It should be possible to discover a Higgs boson with mass greater than about 150 GeV using just the above selection criteria¹⁾ but the observability of Higgs bosons with masses closer to M_W depends critically on the resolution of the detector.

To further enhance the signal-to-background ratio, we count the number of high impact parameter (h.i.p.) tracks in each event. The definition of a h.i.p. track was given in Sec. 2.4. Events are accepted if the number of h.i.p. tracks is at least four. We first consider the case in which the H^0 decays to $b\bar{b}$. The efficiency for signal events to pass the cut on h.i.p. tracks, after all other cuts, is about 92% while for the background it is about 30%. The invariant mass distributions for a 120 GeV Higgs boson and a 150 GeV Higgs boson are shown in Figs. 1(a) and (b), respectively. The figures include standard model backgrounds. The 150 GeV Higgs boson signal is clearly separated from the large W peak due to the $e^+e^- \rightarrow e^+ \nu_e W^-$ background. However, the 120 GeV Higgs boson signal is just a shoulder on the side of the W^\pm mass peak. The 120 GeV signal stands out clearly, though, if the resolution of the hadronic calorimeter is:

$$\frac{\sigma_E}{E} = \frac{35\%}{\sqrt{E}} \text{ GeV}^{1/2} + 2\%$$

instead of

$$\frac{\sigma_E}{E} = \frac{50\%}{\sqrt{E}} \text{ GeV}^{1/2} + 2\%$$

After making the cut on h.i.p. tracks, we are left with a background which is dominated by events in which the W^\pm decays to $t\bar{t}$. It should be noted that if the top quark mass is greater than the W^\pm mass, these events will be absent, significantly reducing the background. On the other hand, if the top quark mass is 40 GeV, the signal-to-noise ratio is improved by about 60% by reducing the allowed jet mass range from (1–50) GeV to (1–25) GeV. However, the number of signal events which pass all of the selection criteria is reduced by about 60%.

For Fig. 1, we assumed that the Higgs boson decays to a bottom quark pair. If we assume that the Higgs boson decays to a top quark pair, we can further increase the signal-to-background ratio by accepting events only if they have at least four clusters found by an algorithm which groups particles until further additions to the group would result in a cluster of particles with invariant mass much greater than the bottom quark mass and less than the top quark mass. The technique does not depend critically on the exact cutoff mass. In Fig. 2, we plot the invariant mass of events with at least four high-impact-parameter tracks and at least four clusters found by the clustering algorithm. The distribution includes a 150 GeV Higgs boson and backgrounds. The W peak from the $e^+e^- \rightarrow e^+ \nu_e W^-$ background has been further reduced so that now the peak signal is over half of the peak background.

We conclude that impact parameter tagging is a useful tool for enhancing the signal of an intermediate mass Higgs boson relative to standard model backgrounds. In addition, if the Higgs boson decays to $t\bar{t}$, the number of low mass clusters provides a useful discriminator between signal and background.

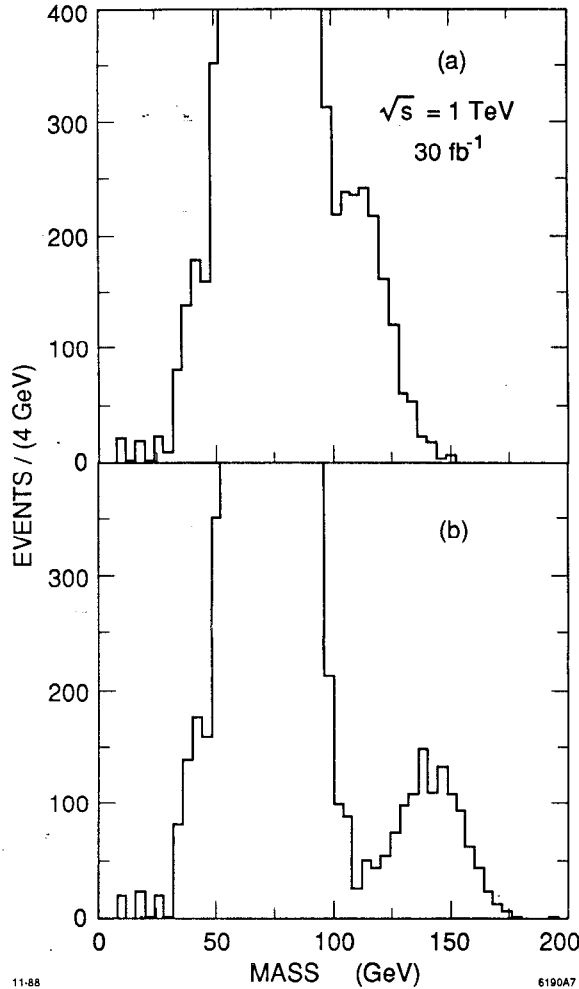


Fig. 1. Reconstructed mass distribution, after selection criteria, for background events plus (a) a 120 GeV Higgs boson and (b) a 150 GeV Higgs boson. The Higgs boson is produced in the process $e^+e^- \rightarrow \nu_e \bar{\nu}_e H^0$ at $\sqrt{s} = 1$ TeV and decays to $b\bar{b}$. The selection criteria include a cut on the number of high-impact-parameter tracks. The number of events in the peak bin near the W^\pm mass is about 3000.

4. MINIMAL HIGGS BOSON AT $\sqrt{s} = 400$ GeV

If the mass of the Higgs boson is less than ~ 200 GeV (for example, $M_{H^0} < 2M_{Z^0}$), the Higgs boson could be discovered and studied at an e^+e^- collider with a center-of-mass energy considerably less than 1 TeV. It is important¹⁰⁾ to gain access to this mass range since it may not be possible to find such particles at any other machine that is currently being contemplated by the particle physics community and because of the difficulty with backgrounds at larger center-of-mass energy discussed in the previous section. We have briefly examined the situation at an e^+e^- collider with $\sqrt{s} = 400$ GeV. The designs of machines¹¹⁾ in this energy range incorporate very little beamstrahlung (the mean energy loss per beam is typically

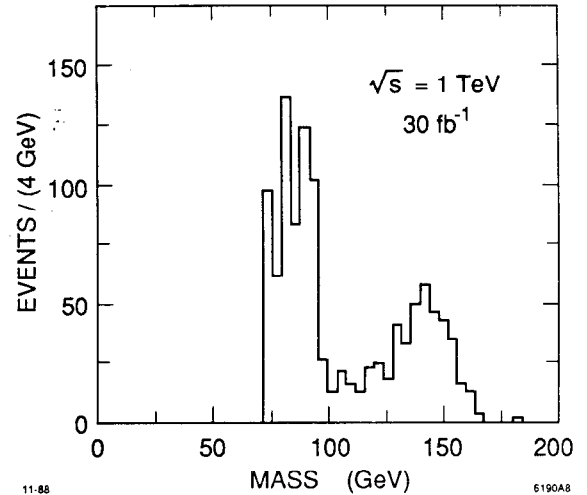


Fig. 2. Reconstructed mass distribution, after selection criteria, for background events plus a 150 GeV Higgs boson. The Higgs boson is produced in the process $e^+e^- \rightarrow \nu_e \bar{\nu}_e H^0$ at $\sqrt{s} = 1$ TeV and decays to $t\bar{t}$. The selection criteria include a cut on the number of high-impact-parameter tracks and on the number of clusters found.

less than a few percent), so analyses that apply energy and momentum constraints are quite efficient.

The cross sections for the processes $e^+e^- \rightarrow Z^0 H^0$ and $e^+e^- \rightarrow \nu_e \bar{\nu}_e H^0$ are shown in Fig. 3 for the case $M_{H^0} = 100$ GeV. The process $e^+e^- \rightarrow Z^0 H^0$ has previously been studied¹²⁾ in detail at $\sqrt{s} = 200$ GeV in preparation for the LEP II physics program. It has been shown that Higgs particles with masses up to 80 GeV can be found rather easily at that machine but that it will be difficult to reach higher masses. The cross section for $e^+e^- \rightarrow Z^0 H^0$ decreases as \sqrt{s} becomes large compared to the masses of the final state particles. However, at $\sqrt{s} = 400$ GeV it is still greater than the fusion reaction $e^+e^- \rightarrow \nu_e \bar{\nu}_e H^0$ for $M_{H^0} = 100$ GeV. There would be approximately 1000 $e^+e^- \rightarrow Z^0 H^0$ events produced in a data sample of 10^6 at this Higgs boson mass. For the machine under discussion, this reaction is clearly worthy of further study.

The decay signatures for $e^+e^- \rightarrow Z^0 H^0$ are summarized in Fig. 4. The analyses of these final states at $\sqrt{s} = 400$ GeV will be quite similar to those developed for LEP II. The process shown in Fig. 4(a) can be isolated from $q\bar{q}$, W^+W^- , and Z^0Z^0 backgrounds at all masses except $M_{H^0} \approx M_{Z^0}$ by taking only high-multiplicity events with large missing transverse momentum. To search for the possibility that the Higgs boson mass is close to that of the Z^0 mass, it is necessary to reduce the Z^0Z^0 background in the sample. This can be done by directly tagging the flavor of the final decay products as discussed in Sec. 2 or by removing events with small sphericity in the center-of-mass system of the observed final state particles as discussed in Ref. (12) Events in which the Z^0 decays to lepton pairs (e^+e^- or $\mu^+\mu^-$) as shown in Fig. 4(b) can be effectively reduced to the same problem once the $Z^0 \rightarrow l^+l^-$ decay has been identified. In this case, the use of the measured

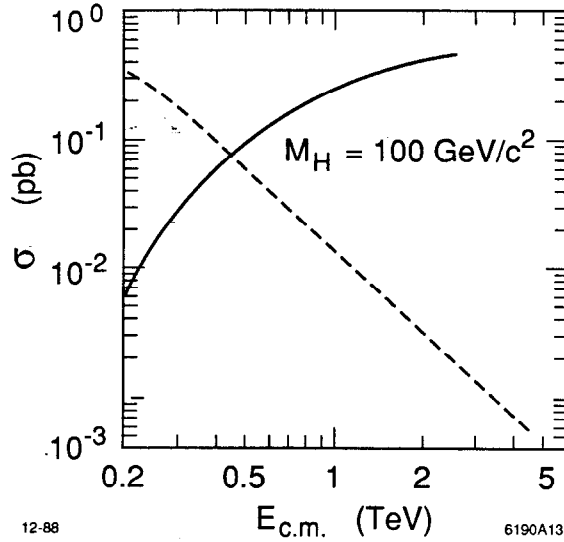


Fig. 3. Cross sections for the processes $e^+e^- \rightarrow Z^0 H^0$ (dashed curve) and $e^+e^- \rightarrow \nu_e \bar{\nu}_e H^0$ (solid curve) for a 100 GeV Higgs boson.

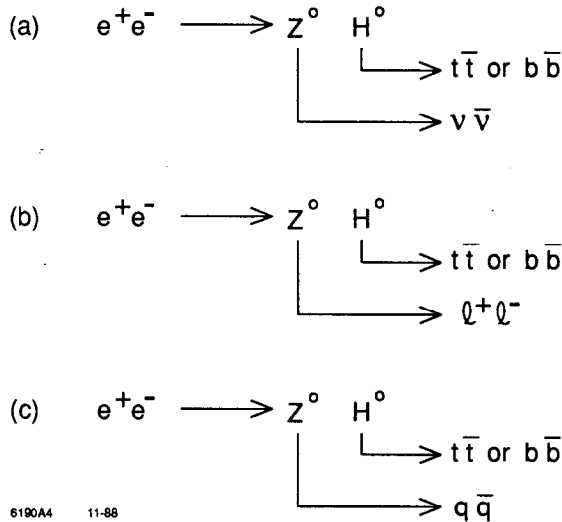


Fig. 4. The decay signatures for the process $e^+e^- \rightarrow Z^0 H^0$.

lepton momenta to reconstruct the Higgs signal as a recoil mass is a useful tool that is available at lower energy e^+e^- machines. We have not done detailed studies of these final states at $\sqrt{s} = 400$ GeV, but Higgs particles with masses up to 180–200 GeV should be visible in these channels.¹³⁾

The hadronic final states shown in Fig. 4(c) are the most numerous, but require the most sophisticated analyses to find and study. The strategy is to reconstruct the individual quark jets. It has been shown¹²⁾ that at LEP II the case $H^0 \rightarrow b\bar{b}$ results in distinctive four-jet events that can be kinematically fitted to yield clear signals for M_{H^0} up to 70 GeV. We consider here the case in which a heavier

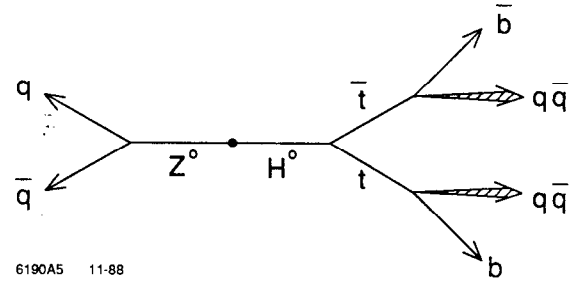


Fig. 5. The jet structure for $e^+e^- \rightarrow Z^0 H^0$ when the Z^0 decays hadronically and the Higgs boson decays to a top quark pair.

Higgs decays to $t\bar{t}$ pairs. For this exercise we assume that the top quark mass is 40 GeV and the parton structure of the final state is as shown in Fig. 5. The signature of this final state is a multijet event tagged by the pair of jets that originate from the decay of the Z^0 . Once this pair has been isolated, the remainder of the event (in its own center-of-mass) is a highly spherical decay of two massive quarks. The details of the event-selection procedure are as follows:

- (1) Reconstruct the visible mass and thrust axis of each event. Demand greater than 300 GeV of visible mass and $|\cos \theta_{thr}| < 0.8$.
- (2) Reconstruct the jet topology of the event. We have used the LUND cluster algorithm modified to find jets with masses only up to 20 GeV. This means that top quarks are split into their decay partons. Require that there be five or more jets in candidate $Z^0 H^0$ events. This technique strongly rejects $Z^0 Z^0$ and $W^+ W^-$ events.
- (3) Search for jet pairs with invariant masses within 15 GeV of the Z^0 mass. If more than one pairing results in a Z^0 candidate, then identify the one with the invariant mass nearest to 93 GeV as the Z^0 . If no candidate Z^0 decays are found, then reject the event.
- (4) Boost to the center-of-mass of the system that recoils against the Z^0 , find the thrust axis in this system, and reconstruct the invariant masses of the observed particles in the hemispheres defined by the plane perpendicular to this thrust axis. Demand that both of these hemisphere masses lie between 20 and 50 GeV as would be expected for decays of 40 GeV top quarks.
- (5) Fit the measured jet four-vectors in each event to the hypothesis that energy and momentum are conserved and that the Z^0 mass is 93 GeV. We have assumed that there is no smearing of the overall center-of-mass energy and momentum due to beamstrahlung, but have included lowest order initial state radiation. Reject events if they yield a poor fit ($\chi^2/DOF > 1$).

The result of this analysis is shown in Fig. 6. Backgrounds from all annihilation and two-photon processes are summed and shown as the open region. The signal is shown as the shaded region. This also includes $Z^0 H^0$ events in which the wrong pair of jets is identified as the Z^0 . The solid histogram gives the signal that would be seen for $M_{H^0} = 150$ GeV. An integrated luminosity of 10 fb^{-1} would result in a signal of 43 events over a background of 35 events.

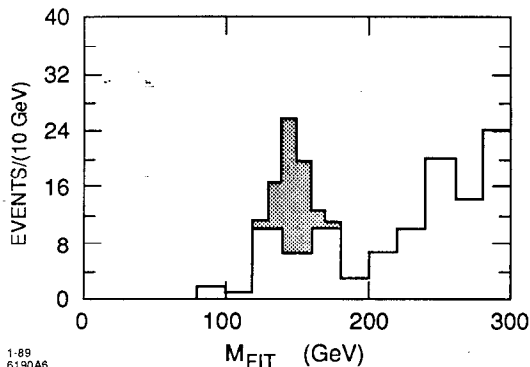


Fig. 6. Invariant mass distribution, after selection criteria, for a 150 GeV Higgs boson produced in the process $e^+e^- \rightarrow Z^0 H^0$ at $\sqrt{s} = 400$ GeV. Backgrounds from annihilation and two-photon processes are shown as the open region; the signal is shown as the shaded region.

We conclude that Higgs boson searches at an e^+e^- collider with $\sqrt{s} = 400$ GeV will be successful in the $Z^0 H^0$ channel for M_{H^0} at least as large as twice the Z^0 mass. The mass interval near M_{Z^0} will require special attention, but the $Z^0 Z^0$ cross section is only ≈ 5 times the $Z^0 H^0$ cross section (when $M_{H^0} = M_{Z^0}$) and the techniques of jet counting and flavor tagging discussed earlier in this paper effectively isolate the heavy quark decays of the Higgs boson. An integrated luminosity of 10 fb^{-1} will suffice to find and conduct reasonable studies of the minimal H^0 . This sample could be accumulated over a 3-4 year period of operation at a machine with an instantaneous luminosity of $\approx 3 \times 10^{32} \text{ cm}^{-2} \text{ s}^{-1}$.

5. NONMINIMAL NEUTRAL HIGGS BOSONS AT $\sqrt{s} = 1 \text{ TeV}$

In the simplest extension of the standard model, two Higgs doublets yield five physical Higgs particles, two charged and three neutral. The neutral Higgs particles consist of two CP-even states (h^0 and H^0) and a CP-odd state (A^0). The masses of the charged and three neutral Higgs bosons, and two mixing angles are free parameters in the most general case. Minimal supersymmetry can be used¹⁴ to impose constraints, reducing the free parameters from six to two. These may be chosen to be the charged Higgs boson mass, M_{H^\pm} , and the ratio of the vacuum expectation values of the two Higgs doublets, expressed as $\tan \beta$. Once M_{H^\pm} and $\tan \beta$ are specified, production cross sections, decay branching ratios, and masses of the neutral Higgs particles can be calculated. The results of Ref. (14) may be summarized briefly. The light scalar h^0 behaves much like the standard model Higgs boson and may be produced by the familiar mechanism $e^+e^- \rightarrow Z^* \rightarrow Zh^0$ with some possibility for discovery at SLC or LEP. By contrast, these production mechanisms are forbidden for the A^0 and suppressed for the H^0 . The only production mechanism available to these heavy Higgs particles that has adequate cross section is $e^+e^- \rightarrow Z^* \rightarrow H^0 A^0$. At 1 TeV, the largest predicted cross section is approximately 10 fb , or about one-tenth the lowest order QED cross section for

$e^+e^- \rightarrow \mu^+\mu^-$. A key challenge for a TeV linear collider is the discovery of the H^0 and A^0 , should they exist. In the remainder of this section, we investigate techniques for such discovery and attempt to evaluate the likelihood of success.

For this study we assume that the charged Higgs mass is 150 GeV, the top quark mass is 60 GeV, and the ratio of the Higgs vacuum expectation values $\tan \beta$ is 1.5. The masses of the neutral Higgs bosons and their decay modes and branching ratios with these assumptions are given in Table 1. We note that $M_{H^0} = 153 \text{ GeV}$, $M_{A^0} = 126 \text{ GeV}$, and the branching ratios are dominated by $t\bar{t}$ and $b\bar{b}$. The choice of 150 GeV for the charged Higgs mass is motivated by two considerations. If $M_{H^\pm} \leq 135 \text{ GeV}$ then $M_{A^0} \leq 100 \text{ GeV}$ and there is little hope of seeing the signal over the W and Z background. As M_{H^\pm} becomes larger than 150 GeV, the signal is further from the W and Z background, and becomes only easier to see. Moreover, for large M_{H^\pm} , $M_{A^0} = M_{H^0}$, giving one additional handle on the signal that may be exploited. The choice of $M_{H^\pm} = 150 \text{ GeV}$ was therefore felt to be the most challenging case with any prospect of success.

Table 1. Parameters used to generate $e^+e^- \rightarrow H^0 A^0$.

$M_{H^\pm} = 150 \text{ GeV}$	$BR(H^0 \rightarrow t\bar{t}) = 79.6\%$
$M_{H^0} = 153.4$	$BR(H^0 \rightarrow b\bar{b}) = 6.5\%$
$M_{A^0} = 125.7$	$BR(H^0 \rightarrow h^0 h^0) = 13.6\%$
$M_{h^0} = 29.2$	$BR(A^0 \rightarrow t\bar{t}) = 95\%$
$M_t = 60$	$BR(A^0 \rightarrow b\bar{b}) = 5\%$
$\tan \beta = 1.5$	$BR(h^0 \rightarrow b\bar{b}) = 100\%$

Events of the type $e^+e^- \rightarrow H^0 A^0$ are characterized by two jets of unknown, and not necessarily equal, mass. To maintain the highest level of generality, the analysis exploits only two features of the events: the fact that the jets should be distributed as $\sin^2 \theta$, and the fact that many b -quarks will be produced, leading to events with high multiplicity and tracks with large impact parameters. The dominant standard model backgrounds are $e^+e^- \rightarrow q\bar{q}$, $e^+e^- \rightarrow W^+W^-$ and $e^+e^- \rightarrow Z^0 Z^0$. In contrast to $H^0 A^0$ events, these backgrounds are characterized by angular distributions peaked in the forward and backward direction, by lower multiplicity, and by few tracks with large impact parameters. The cuts on multiplicity and impact parameter prove to be the most powerful in enhancing the signal-to-background ratio.

In a run of 10 fb^{-1} integrated luminosity, one expects to produce approximately 112 $H^0 A^0$ events, 40000 $q\bar{q}$ events, 35000 W^+W^- events, and 2000 $Z^0 Z^0$ events. To simulate such a run, we generate the correct numbers of background events, and 1120 $H^0 A^0$ events which are then weighted by 0.1. We apply the following cuts:

- (1) The total number of detected charged tracks in the detector volume ($|\cos \theta| \leq 0.9$) is at least 40. This favors events with b -quarks which tend to have high multiplicities.
- (2) The number of detected charged tracks in the central region of the detector ($|\cos \theta| \leq 0.71$) is at least 20. This cut favors events with $\sin^2 \theta$ distribution.

- (3) The total number of high impact parameter tracks (as defined previously) is at least 16. This strongly favors events with b -quarks.
- (4) When the event is divided into two jets by a cluster finding algorithm,¹⁵⁾ then the cluster containing fewer high impact parameter tracks must still contain at least seven such tracks. This tends to reject background events in which one jet has a large number of high impact parameter tracks due to a statistical fluctuation.
- (5) The invariant mass of each jet is formed and the event is rejected if *both* jets have a mass in the range 63 GeV to 112 GeV. This helps reject remaining W^+W^- and Z^0Z^0 events. Naturally it also excludes any possibility of finding H^0A^0 events with masses in this range, but in doing so enhances the prospects for finding such events with masses *near* the W and Z^0 .

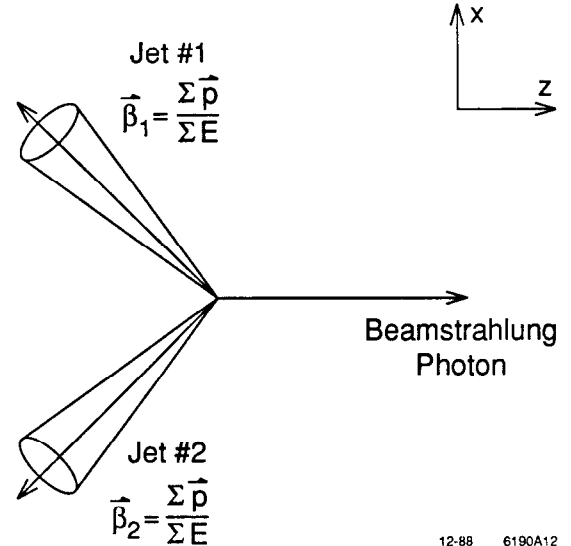
The results of this analysis are not sensitive to the exact number of detected charged tracks required in the first two cuts. The number required would have to be tuned for a particular detector configuration.

Table 2. Selection criteria and number of events which satisfy each criteria.

Cut	H^0A^0	$q\bar{q}$	W^+W^-	Z^0
Generated sample	1120	40000	35000	2000
Total charged multiplicity ≥ 40	774	5934	995	53
Central multiplicity ≥ 20	753	5505	853	45
# High impact parameter tracks ≥ 16	426	128	65	6
# H.i.p. tracks on side with fewer ≥ 7	305	71	32	2
Not both in $63 \text{ GeV} < M < 112 \text{ GeV}$	302	66	14	1

Table 2 shows the impact of each of these cuts on the signal and background events. The net efficiency for the H^0A^0 signal is 27% and the rejection power against standard model backgrounds is approximately 1000:1. For a 10 fb^{-1} run we expect 30 signal and 81 background events, giving an overall signal-to-background ratio of about 1:3. A nonstandard-model background which we do not address here is the process $e^+e^- \rightarrow \gamma^*, Z^* \rightarrow H^+H^-$ which is expected to have a cross section approximately three times larger than the H^0A^0 cross section. Such events will pass our selection criteria. In the minimal supersymmetric model, it is predicted that $M_{H^\pm} \sim M_{H^0} \sim M_{A^0}$ as the mass of the charged Higgs particle becomes heavier ($M_{H^\pm} \gtrsim 150 \text{ GeV}$). For such a case, it would be very difficult to distinguish the Higgs particles from one another unless some new characteristic parametrization other than the invariant mass is found. Outside the context of supersymmetry, however, no relation among the Higgs masses is predicted and the mass peaks need not be close to one another at all.

The invariant masses of the clusters are calculated with a beam energy constraint included. The beam-constrained mass calculation balances the momentum of the two clusters and the (unobserved) beamstrahlung photon in both the beam direction and the plane transverse to the beam direction, and requires in addition that the three energies sum to 1 TeV. By making the approximation that all beamstrahlung and initial state radiation is carried by a single photon, we can write the momentum and energy conservation conditions as three equations in three variables (the two cluster energies and the beamstrahlung photon energy). The invariant masses of the clusters are then computed using the beam-constrained cluster energies. Figure 7 shows the configuration of the two-jet momenta and the beamstrahlung momentum. In general, the three vectors do not lie in a plane as shown in Fig. 7, but a (small) Lorentz boost transverse to the beam direction is applied to bring them into this configuration. We then compute the velocity vector for each jet by summing over particle momenta and energies: $\beta = \Sigma p_i / \Sigma E_i$. In the coordinate system shown in Fig. 7, the momentum and energy constraint equations become



12-88 6190A12

Fig. 7. Momentum vectors for two jets and a beamstrahlung photon. The z -axis is along the beam direction.

$$\beta_{1z}E_1 + \beta_{2z}E_2 = 0 \quad ,$$

$$\beta_{1z}E_1 + \beta_{2z}E_2 + P_\gamma = 0 \quad , \quad \text{and}$$

$$E_1 + E_2 + E_\gamma = \sqrt{s} \quad .$$

In the approximation that only one photon carries away momentum and energy, we have $E_\gamma = |P_\gamma|$. Solving for E_1 , E_2 , and E_γ , we then derive the jet masses using $M_i = E_i \sqrt{1 - \beta_i^2}$. The beamstrahlung photon energy E_γ is a by-product of little direct use, but it is checked against the generated energy to confirm the correctness of

the method. Use of the algorithm sharpens the mass distributions and yields mass values quite close to the generated values. It proves to be essential for identification of mass peaks above background. The method is generally useful for analysis of two-jet events with missing momentum and energy along the beam axis.

Figures 8 (a) and (b) show the mass distributions for the higher mass cluster and the lower mass cluster, just prior to applying the final analysis cut (exclusion of events with both masses in the range 63–112 GeV). A substantial background of W and Z events is evident. Figures 9(a) and (b) show the same plots after all analysis cuts are applied. In Fig. 9(a) the higher mass cluster stands out clearly at the correct (*i.e.* generated) mass of ~ 150 GeV while in Fig. 9(b) the lower mass cluster (expected at ~ 125 GeV) is obscured by the presence of W^\pm and Z^0 backgrounds. The lower mass cluster may be enhanced by applying a cut on the higher mass cluster. Figure 10(a) shows that when the higher mass is required to lie inside the range 120–200 GeV, a choice motivated by Fig. 9(a), the lower mass cluster stands out more clearly. By contrast, Fig. 10(b) shows the lower mass cluster distribution when the higher mass is required to lie *outside* the range 120–200 GeV; in this case there is no evidence for a mass peak.

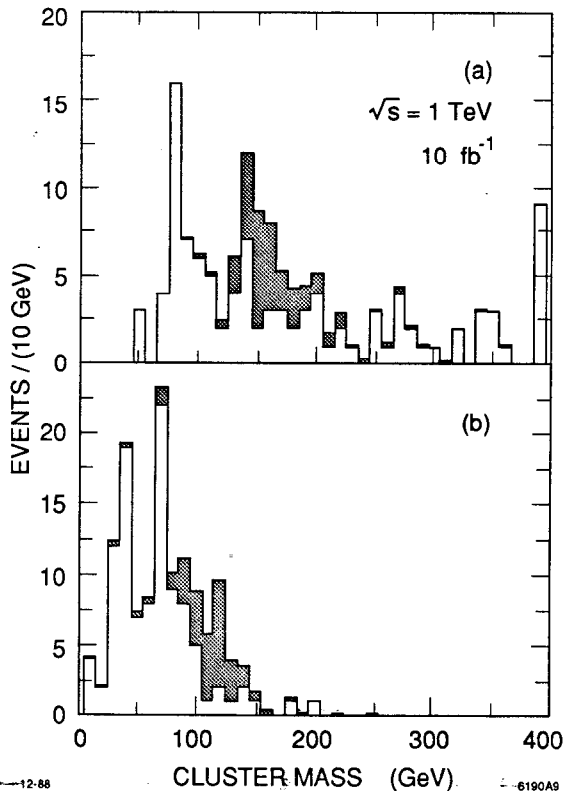


Fig. 8. Reconstructed mass distribution for (a) the larger mass cluster and (b) the smaller mass cluster when the final analysis cut (exclusion of events with both masses in the range 63–112 GeV) is not applied. The shaded region is signal; the open region is background.

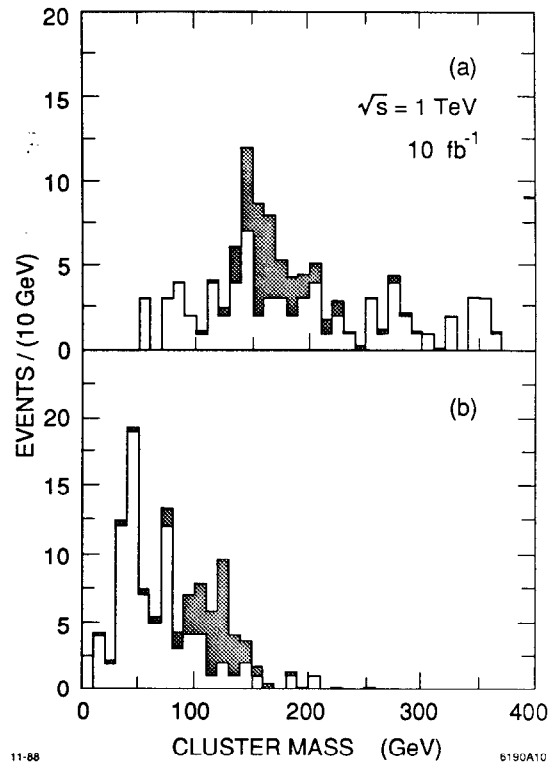


Fig. 9. Reconstructed mass distribution for (a) the larger mass cluster and (b) the smaller mass cluster when all analysis cuts are applied. The shaded region is signal; the open region is background.

We conclude that with modest impact parameter resolution and simple cuts designed to enhance events with b -quarks and central distributions, a sample of 10 fb^{-1} integrated luminosity is sufficient to identify the presence of $H^0 A^0$ events with Higgs boson masses larger than ~ 110 GeV and with decay modes dominated by heavy quarks.

6. CHARGED HIGGS BOSON AT $\sqrt{s} = 1 \text{ TeV}$

6.1 Introduction

Charged Higgs bosons can be produced in pairs in e^+e^- annihilation via a virtual photon, or via a real or a virtual Z boson. The cross section normalized to the lowest order QED cross section for muon pairs, $R(H^+H^-)$, does not depend strongly on the models except near the Z peak since the photon couples to all charged particles with the same strength. In a previous study,²⁾ it was demonstrated that searches for charged Higgs bosons at e^+e^- colliders with $\sqrt{s} \approx 1/2 - 1 \text{ TeV}$ are relatively easy. The main conclusions from the earlier study are:

- (1) With an e^+e^- linear collider of $\sqrt{s} \approx 1/2 - 1 \text{ TeV}$ and an integrated luminosity of about 10^{40} cm^{-2} , we can detect production of charged Higgs bosons and determine the mass for H^\pm bosons with masses less than 80% of the beam energy and a dominant decay mode $H^+ \rightarrow t\bar{b}$. we can detect production of charged Higgs bosons and determine the mass for H^\pm bosons with masses less than 80% of the beam energy and a dominant decay mode $H^+ \rightarrow t\bar{b}$.

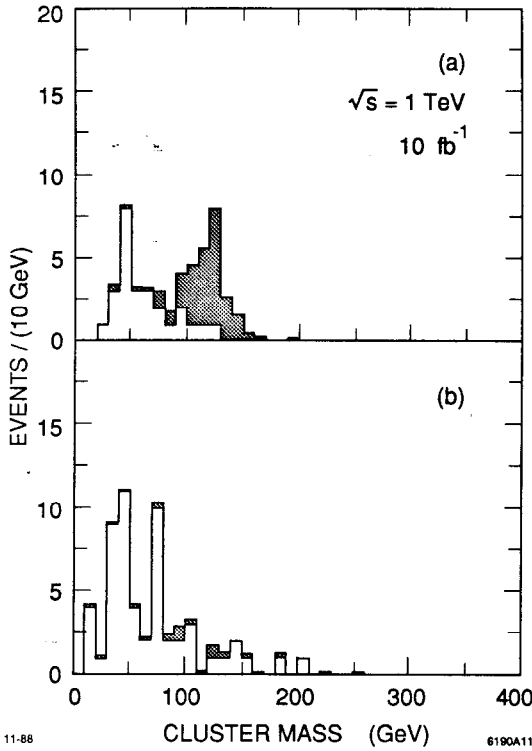


Fig. 10. Reconstructed mass distribution of the smaller mass cluster for events in which (a) the larger mass lies inside the range 120–200 GeV and (b) the larger mass lies outside the range 120–200 GeV. The shaded region is signal; the open region is background.

- (2) If the charged Higgs boson is sufficiently lighter than the top quark, the top quark decays to H^+b . We can then detect the signal of the charged Higgs boson both through its direct pair production and in the top quark decay.
- (3) If there is a light neutral Higgs boson, a charged Higgs boson may decay into W plus the neutral Higgs boson with a large branching fraction. Even if neutral Higgs bosons cannot be produced via the process $e^+e^- \rightarrow Z^0 H_i^0$, or WW - or ZZ -fusion (for example, the CP-odd state), the neutral Higgs boson can be produced and detected in the decay $H^\pm \rightarrow W^\pm H_i^0$.
- (4) It is necessary to understand higher order QCD processes, to improve the QCD shower models, and to test them at lower energies. Also, processes containing weak vector bosons must be experimentally understood.
- (5) Beamstrahlung effects must be moderate. We have to compromise between the integrated luminosity and beamstrahlung effects. The moderate beamstrahlung effects assumed in the earlier Monte Carlo studies²⁾ are perfectly acceptable for studies of charged Higgs boson production.

However, it looks difficult to search for H^\pm if the mass is close to the W^\pm mass since some of the W boson decay modes are the same as the H^\pm decay modes and the cross section for W^\pm production is about 100 times larger than for H^\pm production. Fortunately, since the W^+W^- differential cross section peaks in the forward region and is relatively low in the backward region, we can efficiently reduce the background by rejecting events in the forward region if the charge of the W can be identified. Even if we cannot measure the charge, we can reduce the W pair background by applying a hard cut on the polar angle: for example, $|\cos\theta| < 0.5$. Although W bosons have the same decay modes as charged Higgs bosons, their branching fractions are very different since charged Higgs bosons prefer to couple to heavy fermions ($t\bar{b}$, $c\bar{s}(\bar{b})$ or $\nu_\tau\tau^+$) while W bosons couple to all fermions with the same strength.

We can also search for the charged Higgs boson in top quark decay. We have already studied this case in the previous paper²⁾ and the analysis does not depend significantly on the H^\pm mass (of course, the H^\pm mass must be lighter than the top quark mass). Therefore, we do not repeat the analysis in this report.

In the next section, we will demonstrate that we can find H^\pm at TeV e^+e^- colliders with an integrated luminosity of 10 fb^{-1} even if the H^\pm mass is very close to the W^\pm mass.

6.2 $M_{H^\pm} > M_t + M_b$

For this case, the production and decay sequence is $e^+e^- \rightarrow H^+H^- \rightarrow t\bar{b} + b\bar{t}$. These events have approximately a two-jet structure for $M_{H^\pm} = 70\text{--}100 \text{ GeV}$ at $\sqrt{s} = 1 \text{ TeV}$. To enhance the H^+H^- signal relative to WW and ZZ backgrounds, and ordinary multihadron backgrounds, the following cuts are applied (the cuts are optimized for $M_{H^\pm} \approx M_W$ and $\sqrt{s} = 1 \text{ TeV}$):

- (1) $E_{\text{vis}} > 0.5\sqrt{s}$, where E_{vis} is the total visible energy measured by the electromagnetic and hadronic calorimeters (muon momenta are added).
- (2) $|\Sigma p_z|/E_{\text{vis}} < 0.4$, where Σp_z is the sum of the longitudinal momenta measured in the same way as the visible energy.

Cuts (1) and (2) reject events with large momentum imbalance along the beam direction due to beamstrahlung and initial state radiation.

- (3) $|\cos\theta_{\text{thr}}| < 0.50$, where θ_{thr} is the polar angle of the thrust axis.

This cut rejects the major part of the W^+W^- background. The event is now divided into two hemispheres by the plane perpendicular to the thrust axis.

- (4) Both thrust hemispheres must have large numbers of charged particles: one hemisphere must have at least 16 charged particles and the other must have at least eight.

Since in each event there are four B -hadrons which have a relatively long lifetime of about 1 ps, we select events containing many charged particles with large impact parameter. For this analysis, we assume an impact parameter resolution of

$$\sigma_\delta = \sqrt{(10 \text{ } \mu\text{m})^2 + [70 (\text{ } \mu\text{m GeV})/p]^2}$$

The following cut is then applied:

- (5) The number of charged tracks with large impact parameter δ in each thrust hemisphere is counted. Only events with many large-impact-parameter tracks in both thrust hemispheres are selected: one thrust hemisphere must have at least five such tracks and the other must have at least three. The definition of a large-impact-parameter track for this analysis is: $p > 1$ GeV, $\delta/\sigma_\delta > 3$, and $\delta < 2$ mm. The larger impact parameter cut of 2 mm reduces the contamination of charged particles from K_S or Λ decays.
- (6) The difference in the invariant mass of each hemisphere must be less than 15 GeV.

After all the cuts, the reconstructed Higgs mass (the average of the two hemisphere invariant masses in an event) is plotted for $M_{H^\pm} = 70$ GeV, 83 GeV, 93 GeV and 100 GeV in Fig. 11(a)-(d). Contributions from the background processes WW , ZZ and $q\bar{q}$ are added to the plots. As can be seen from the plots, the signal (shaded part in the figure) is larger than the background near M_{H^\pm} . The plots are normalized to an effective integrated luminosity of 10 fb^{-1} .

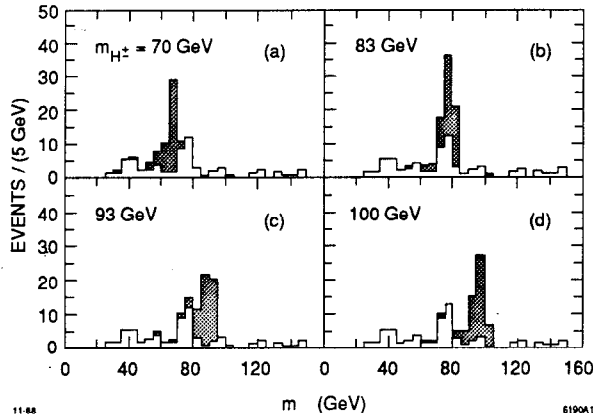


Fig. 11. Invariant mass distribution of reconstructed charged Higgs bosons (the average of the two in each event) after all the cuts for $H^+H^- \rightarrow b\bar{t}t\bar{b}$ with (a) $M_{H^\pm} = 70$ GeV, (b) $M_{H^\pm} = 83$ GeV, (c) $M_{H^\pm} = 93$ GeV, (d) $M_{H^\pm} = 100$ GeV. The top quark mass is assumed to be 60 GeV. The shaded region is signal; the open region is background.

6.3 $M_{H^\pm} < M_t + M_b$

If the decay $H^- \rightarrow b\bar{t}$ is kinematically forbidden, it is worth studying events of the type $\tau^- \bar{\nu}_\tau + \text{hadrons}$ since the branching fraction for the decay mode $H^- \rightarrow \tau^- \bar{\nu}_\tau$ can be as large as 30%. The branching fraction depends only on the ratio of the vacuum expectation values for the minimal supersymmetric model, and in general it depends on the Higgs boson-fermion couplings and Higgs boson-gauge boson couplings. Therefore, we will study the production and decay sequence $e^+e^- \rightarrow H^+H^- \rightarrow \tau^+\nu_\tau + s\bar{c}(b\bar{c})$.

The cuts to select $H^+H^- \rightarrow \tau\nu + \text{hadrons}$ are the following:

- (1) $N_{ch} \geq 3$ where N_{ch} is the number of visible charged particles.
- (2) $E_{vis} > 0.5 \sqrt{s}$.

- (3) $|\Sigma p_z|/E_{vis} < 0.4$.

- (4) One of the thrust hemispheres (hemisphere 1) is required to have exactly one charged particle. The momentum of this particle must be greater than 5 GeV. The invariant mass of this hemisphere M_1 is required to be less than 5 GeV. The invariant mass of the other thrust hemisphere M_2 must be larger than 50 GeV and the charged multiplicity N_{ch2} must be larger than 10; i.e., $N_{ch1} = 1$, $N_{ch2} > 10$, $M_1 < 5$ GeV, and $M_2 > 50$ GeV.
- (5) Since the WW background is relatively small in the backward region, the events are restricted to this region. The event must satisfy $0.0 < Q_1 \cos \theta_{thr} < 0.7$ where Q_1 is the charge of the single particle in hemisphere 1 and θ_{thr} is the direction of the thrust axis pointing out of hemisphere 1.

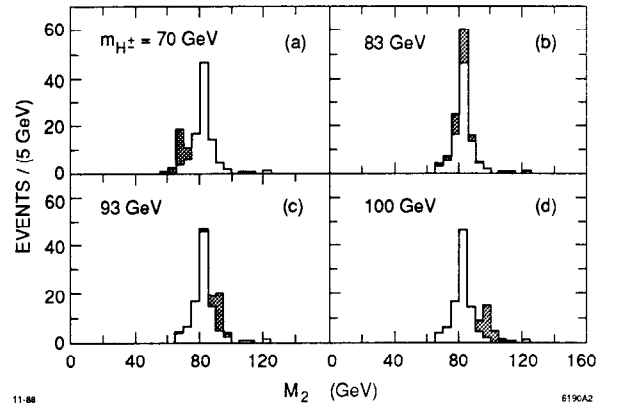


Fig. 12. Distribution of the larger hemisphere mass after cuts (1) to (5) for $H^+H^- \rightarrow \tau\nu + \text{hadrons}$ (shaded region) in addition to the expected background (open region) for (a) $M_{H^\pm} = 70$ GeV, (b) $M_{H^\pm} = 83$ GeV, (c) $M_{H^\pm} = 93$ GeV, and (d) $M_{H^\pm} = 100$ GeV.

After applying cuts (1)-(5), the higher hemisphere mass M_2 is plotted for $M_{H^\pm} = 70$ GeV, 83 GeV, 93 GeV and 100 GeV in Fig. 12 (a)-(d). Contributions from the background processes WW , ZZ and $q\bar{q}$ are added in the plot. The dominant background due to $e^+e^- \rightarrow W^+W^-$ events makes it difficult to see the signal close to the W^\pm mass. In Fig. 13, the same plots are shown for the case when the charged particle in hemisphere 1 is a pion. We assume 100% efficiency for pion identification and no particle misidentification. The signal-to-background ratio is improved because of the large branching fraction for $\tau^- \rightarrow \nu_\tau \pi^- + n\pi^0$ ($n \geq 0$). A branching fraction of 30% for $H^- \rightarrow \tau^- \bar{\nu}_\tau$ is assumed in this analysis. The plots are normalized to an integrated luminosity of 10 fb^{-1} .

6.4 Summary

Charged Higgs bosons with a mass of 70-100 GeV can be found at e^+e^- colliders with $\sqrt{s} \sim 1$ TeV with an integrated luminosity of $O(10^{40} \text{ cm}^{-2})$, even if the mass is very close to the W mass. The event topology $H^+H^- \rightarrow t\bar{b} + b\bar{t}$ can be selected by using the b -tagging method in addition to a hard polar angle cut which rejects WW background.

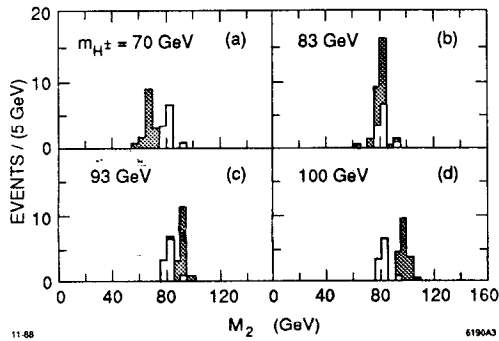


Fig. 13. Distribution of the larger hemisphere mass after requiring the isolated particle to be a charged pion for $H^+H^- \rightarrow \tau\nu + \text{hadrons}$ events (shaded region) in addition to the expected background (open region) for (a) $M_{H^\pm} = 70$ GeV, (b) $M_{H^\pm} = 83$ GeV, (c) $M_{H^\pm} = 93$ GeV, and (d) $M_{H^\pm} = 100$ GeV.

The process $H^+H^- \rightarrow \tau\nu + cs(cb)$ can be selected by tagging an isolated pion from the tau decay and by rejecting events in the backward region where WW backgrounds dominate.

These methods can also be used at intermediate energy (350–400 GeV) e^+e^- colliders. At $\sqrt{s} = 400$ GeV, the signal-to-background ratio is worse than at 1 TeV because the relative cross section of H^+H^- to W^+W^- is smaller due to the different threshold behavior of the two processes. On the other hand, the absolute cross section for the signal is larger at lower energies.

At LEP II it may be difficult to detect a charged Higgs boson with mass around the W mass with a luminosity of 500 pb^{-1} . The R value for a 83 GeV H^\pm at $\sqrt{s} = 200$ GeV is only 0.057, so the number of expected events after cuts is very small and the W background is larger. At LEP energies, the event topology is not two back-to-back jets and the particles from H^+ and H^- will be mixed with each other due to the small velocity of the H^\pm . Therefore, a more complicated analysis may be required. In any case, the b -tagging and the polar angle cuts discussed in this report are useful at any energy.

7. CONCLUSIONS

High energy e^+e^- colliders will offer nearly ideal opportunities to search for and study the Higgs sector of nature or its equivalent.¹⁶⁾ We have shown that at $\sqrt{s} = 1$ TeV the neutral Higgs boson that appears as a real particle in the simplest doublet model of the Higgs sector can be clearly isolated as long as its mass is less than about 80% of the beam energy and greater than about 120 GeV. Near the mass of the W^\pm , the tagging of high-impact-parameter tracks is an important tool for enhancing the signal-to-background ratio. The intermediate mass range ($M_{H^0} \lesssim 2M_{Z^0}$) can be reached at $\sqrt{s} \approx 400$ GeV. We study the case in which the Higgs boson is heavy enough to decay to $t\bar{t}$. In this case, the reconstruction of parton jets is an important tool for rejecting backgrounds.

Models in which the Higgs sector is more complicated contain greater numbers of new particles which can be found and studied. We have determined that charged Higgs particles can be found even when the mass is near the W^\pm mass and that the neutral members of the spectrum of Higgs states can be seen over a limited mass range in some models through the production mechanism $e^+e^- \rightarrow H^0 A^0$. Again, the tagging of high-impact-parameter tracks is essential for identifying the neutral Higgs bosons.

Integrated luminosities of $(10\text{--}30) \text{ fb}^{-1}$ are needed to complete the investigations that we have discussed. Beamstrahlung is not a major problem for most analyses and at lower energy machines ($\sqrt{s} \lesssim 500$ GeV) the design parameters that have been proposed do not predict significant beamstrahlung in any case. The requirements that are placed on detectors are quite modest and can be satisfied with existing technology.

REFERENCES

1. Burchat, P. R., Burke, D. L., and Petersen, A., Phys. Rev. **D38**, 2735 (1988). After publication an error was found in the simulation of detector resolution. After correcting the error, the W mass peak from $e^+e^- \rightarrow e^+ \nu_e W^-$ is approximately twice as wide as reported, dominating the Higgs boson signal from $e^+e^- \rightarrow \nu_e \bar{\nu}_e H^0$ for a Higgs mass less than about 150 GeV. The error has no significant effect on the heavy Higgs boson analysis. The correct simulation is used for this Snowmass study.
2. Komamiya, S., Phys. Rev. **D38**, 2158 (1988).
3. Yokoya, K., Nucl. Instrum. Methods **A251**, 1 (1986); Chen, P., SLAC-PUB-4293, 1987.
4. Palmer, R. B., SLAC-PUB-4295 (1987); Schnell, W., *Advanced Accelerator Concepts*, Madison, WI, AIP Conf. Proc. **156**, 12 (1987), and SLAC/AP-61 (1987).
5. Sjostrand, T., and Bengtsson, M., Computer Phys. Comm. **43**, 367 (1987).
6. Gabrielli, E., ROME-550-1987.
7. Feldman, G. J., SLAC-PUB-4563, 1988.
8. Richard, F., Proc. of the Workshop on Physics at Future Accelerators, La Thuile (Italy) and Geneva (Switzerland), January 7–13, 1987; Mele, B., *ibid.*
9. Yehudai, E., private communication.
10. Kane, G. L., and Scanio, J. J. G., CERN-TH.4532/86, 1986.
11. Palmer, R., and Ruth, R., contributions to these proceedings.
12. Boucrot, J. *et al.*, CERN-EP/87-40, 1987.
13. Grosse-Wiesmann, P., these proceedings.
14. Gunion, J. F. *et al.*, Phys. Rev. **D38**, 3444 (1988).
15. Bartel, W. *et al.*, Z. Phys., **C33**, 23 (1986).
16. "New Particle Searches in e^+e^- Collisions," report of study group, these proceedings.